JOURNAL OF MATERIALS SCIENCE 17 (1982) 2424–2430

Crystal growth of Ti_nO_{2n-1} oxides ($n = 2$ to 9)

PIERRE STROBEL, YVON LE PAGE
Solid State Chemistry, National Research Council of Canada, Ottawa K1A 0R9, Canada

Crystals of titanium oxides, Ti_nO_{2n-1} with $n = 2$ to 9, were grown by chemical vapour transport. Chlorine was found to be the best transporting agent. Apart from Ti_2O_3, for which crystals up to 7 mm long were obtained in 6 days, all phases were obtained in conditions leading to very low growth rates and a shift in composition between the charge and growth zones. It is shown that this shift is governed by the equilibrium oxygen pressure in the transport tubes and can be accurately predicted. Most of the millimetre-size samples obtained were twinned.

1. Introduction

The titanium–oxygen system contains numerous phases with remarkable properties. Between metallic $Ti^{II}O$ and insulating $Ti^{IV}O_2$ (rutile), titanium forms a series of oxides with the general formula Ti_nO_{2n-1} ($n \geq 2$), which exhibit semiconductor–metal transitions [1]. This series includes corundum-type Ti_2O_3 and the "Magneli phases" Ti_nO_{2n-1} ($n \geq 3$), with titanium valencies intermediate between 3 and 4. Apart from monoclinic Ti_3O_5, these phases are closely related structurally. They are built of rutile-like slabs which extend infinitely in two dimensions, but are only n TiO_6 octahedra thick perpendicular to a shear plane, where octahedra share faces in addition to edges and corners [2]. Two distinct families are found where the shear planes are either (121) (for $n = 4$ to 9) or (132) (for $n \geq 16$) [3]. Both families are triclinic.

Physical studies of these materials have been restricted so far to the members of the series with $n = 2$ to 5 [1, 4–6], mainly because of the difficulty of obtaining large single crystals. Two growth techniques have been used. The first crystals were grown by Bartholomew and White [7] using a flux method under controlled oxygen pressure. In addition to Ti_2O_3, which is easy to grow [8, 9], several authors grew oxides with $n = 3$ to 5 by chemical vapour transport, using $TeCl_4$ or NH_4Cl as a transporting agent [10–12]. Recently Bando *et al.* [13] succeeded in growing single crystals of Ti_nO_{2n-1} with large values of n (12 to 20) by chemical vapour transport. A high-temperature thermodynamic study of the Ti–O–Cl system is also available [14], but it concluded that no Magneli phases with $n > 4$ should be obtained by chemical transport, in contradiction to previous experimental results. The present article reports the results of a systematic study of the crystal growth of titanium oxides Ti_nO_{2n-1} with $n = 2$ to 9. The growth of Ti_9O_{17}, which had not been grown in single-crystal form before, has been described briefly in a previous paper [15]. The thermodynamic conditions and the parameters for chemical vapour growth are discussed.

2. Thermodynamic considerations

2.1. Oxygen pressure

A striking result of previous vapour transport growth of Ti_nO_{2n-1} oxides with $n \geq 3$ is that, in all cases, the composition of the crystals was different from that of the starting material. The n value in the crystals was frequently higher than expected, indicating additional oxidation, which has been attributed to traces of oxygen or water introduced in the chemical transport process either by the silica tube walls or by the reagents [12, 13]. Thus the oxygen pressure in equilibrium with the depositing crystalline phase is a critical parameter in the crystal growth of the Magneli phases. The equilibrium oxygen pressure, P_O, over titanium oxides has been determined by several authors and is summarized in Fig. 1. It can be seen that, as n is increased, the homogeneity range of each successive phase is narrowed. Consequently, it is increasingly difficult to control the stoichiometry of the depositing solid phase.

0022–2461/82/082424–07$03.34/0

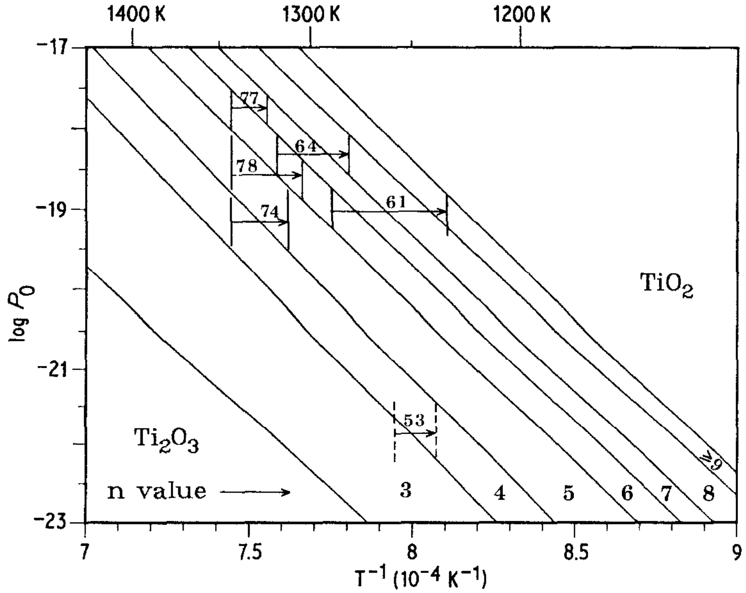

Figure 1 Temperature variation of the equilibrium oxygen pressure (in atm), P_O, above Ti_nO_{2n-1} phases (data from [7]). The vertical bars correspond to experimental conditions of runs in Table II (see Section 5.1).

Small variations in P_O can result in the intergrowth of neighbouring phases, and hence in inhomogeneous crystals for high values of n [13].

2.2. Transport rate

The variation of n in the series Ti_nO_{2n-1} is reflected in the thermodynamic functions of the successive phases, which in turn determine the efficiency of the chemical transport process. An increase in n corresponds to a thickening of the pseudo-rutile slabs and to a decrease in the density of face-sharing octahedra in the structure. Accordingly, the enthalpy and free energy of formation of the oxides decrease when n increases, approaching values for the end number ($n = \infty$) TiO_2 (see Table I).

Bando *et al.* [13] determined the composition of the vapour phase during the transport by mass spectrometry and found that, in agreement with previous theoretical calculations [14], the main titanium species in the vapour is $TiCl_4$. In the simple case of transport by chlorine, the transport reaction can then be written:

$$TiO_x(s) + 2Cl_2(g) \rightleftarrows TiCl_4(g) + \frac{x}{2}O_2(g) \tag{1}$$

where $x = (2n - 1)/n$. The calculated values of the equilibrium constant, K_p, for Reaction 1, listed in Table I, show a steep decrease as n increases. One can therefore expect a decrease in the conversion rate of solid TiO_x into gaseous $TiCl_4$, i.e., a decrease in transport rate as n increases (TiO_2, with $K_p < 10^{-4}$ at 1300 K, is not transported at all).

3. Experimental procedure

3.1. Growth conditions

All experiments were carried out in a calibrated

TABLE I Thermodynamic data for chemical transport at 1300 K: ΔG_F is the free energy of formation of the oxides Ti_nO_{2n-1}; ΔG_r and K_p are the free energy and equilibrium constant for the transport Reaction 1

Oxide	n	ΔG_F (kJ per mol Ti)	ΔG_r (kJ per mol Ti)	K_p (atm)$^{-1/2n}$
$TiO_{1.50}$	2	−582.3	−24.4	9.6
$TiO_{1.67}$	3	−629.7	+22.0	1.3 10^{-1}
$TiO_{1.75}$	4	−650	+43.3	1.8 10^{-2}
$TiO_{1.80}$	5	−663.0*	+56.3	5.4 10^{-3}
$TiO_{1.83}$	6	−671.0*	+64.3	2.6 10^{-3}
$TiO_{1.86}$	7	−676.5*	+69.8	1.6 10^{-3}
$TiO_{1.88}$	8	−680.7*	+74.0	1.1 10^{-3}
$TiO_{1.89}$	9	−683.8*	+77.2	7.9 10^{-4}
TiO_2	∞	−710	+103	7.3 10^{-5}

*Data from [16] (at 1304 K); all other data are from [17].

two-zone furnace with adjustable temperature profile, and two independent temperature controllers with an accuracy better than 0.2%. The precision was within ± 2 K on the temperature of the hot zone and ± 5 K on the temperature of the cold end of the transport tubes, which was more dependent on the length and position of the tubes in the furnaces.

The procedure and conditions of growth of Ti_9O_{17} crystals have been described elsewhere [15]. Similar conditions were applied to other compositions, using an initial charge of Ti + TiO_2 reacted *in situ* in carefully outgassed transport tubes. Chlorine and tellurium tetrachloride were used as transporting agents. The handling of $TeCl_4$, which is a highly corrosive and hydrolizable compound (i.e., a potential source of additional water vapour in the transport process) was avoided by the direct introduction of elemental high-purity tellurium and gaseous chlorine in the transport tubes. Numerous runs were carried out in order to establish the influence of the nature and concentration of transporting agent, the temperature range and gradient, and the back-transport step. The latter, which is a standard procedure in chemical vapour transport to clean the growth zone of any unwanted nuclei, has been reported [12] to cause the release of significant amounts of adsorbed water vapour and an increase of the value of n in the crystals grown.

3.2. Characterization of the crystals

The indentification of the various members of the series Ti_nO_{2n-1} is not simple. From n = 4 to n = 9 (i.e., for a family of Magneli phases with an identical shear plane direction), the strong lines of the X-ray powder pattern occur at similar 2θ angles. Since *et al.* [12] discussed various physical criteria which allow these phases to be distinguished, the most selective being electron spin resonance (ESR). Unfortunately, the ESR spectra are known only for the phases with $n \leqslant 5$.

Bando *et al.* [13] used electron diffraction. We identified all titanium Magneli phases here by single-crystal orientation from known cell data [2], using a 4-circle diffractometer with MoKα radiation. Oscillation photographs around the three crystallographic axes were then taken to avoid ambiguity. Multiple crystals could also be identified as follows: a pair of reflections issuing from the same crystallite was found and entered in the algorithm used above, which requires only two observed reflections in addition to cell data [18]. The period along the reciprocal z^*-axis was then used as a criterion to check the value of n in the crystallite.

4. Results

The experimental conditions and results of chemical vapour transport runs yielding crystals of Ti_nO_{2n-1} with $n = 2$ to 9 are summarized in Table II. The following general trends can be pointed out.

(a) The nature and concentration of the transporting agent have little influence on the growth process (compare Runs 47, 49 and 53); $TeCl_4$ proved to be rather less efficient than Cl_2 for the transport of Ti_2O_3; it was not used here for further runs.

(b) No significant change in the values of n was observed whether back transport was included or not, but it must be stressed that the growth zone of the transport tubes had been thoroughly outgassed in a temperature range near the softening point of silica glass before sealing.

(c) There is a striking difference of behaviour between Ti_2O_3 and the Magneli phases: Ti_2O_3 is transported "normally", without appreciable shift in composition, whereas for all other runs the n value in the crystals was higher than in the charge. Moreover, the transport rate of Ti_2O_3 is approximately an order of magnitude higher than that of the Magneli phases in the presence of chlorine; thus large crystals (up to 6 mm × 7 mm plates) of Ti_2O_3 were obtained in 6 days, to be compared to 3 mm maximum length of Magneli phase crystals obtained in 20 to 25 days.

(d) In all cases, nucleation and growth of single crystals of appreciable size took place in the charge zone, where it was not expected.

Crystals of Ti_2O_3 and Ti_3O_5 were easily recognizable by their habit or colour. Ti_2O_3 (Fig. 2) grew as blue-black hexagonal plates perpendicular to the corundum z-axis. Ti_3O_5 has a characteristic copper-red colour. It forms rectangular plates showing numerous parallel striations separating domains up to 0.2 mm wide (Fig. 3). X-ray diffraction showed that these lines are parallel to [010] and are traces of (001) twin planes.

All higher members of the series were obtained as blue-black tabular or columnar crystals (see Figs 4 to 6). Most samples were twinned, especially

TABLE II Growth conditions and results for Ti_2O_3 to Ti_9O_{17} (T_1 and T_2 are the temperatures of the charge growth zones, respectively).

Run no.	Starting composition	Transporting agent	T_1 (K)	T_2 (K)	Duration (days)	Transport rate (mg day^{-1})	n in crystals		Size of crystals at T_2
							At T_1	At T_2	
57	$TiO_{1.48}$	$TeCl_4$ 1.4 g l^{-1}	1320	1206	6	3.4	2 + 3	2	plates 2 mm × 2 mm
58	$TiO_{1.50}$	Cl_2 41 kPa	1320	1225	6	11.0	2 + 3	2	plates 7 mm × 6 mm
53	$TiO_{1.67}$	$TeCl_4$ 2.1 g l^{-1}	1258	1238	9	very small	3 + 4*	4	prisms of plates 2 mm (mostly twinned) at T_1 : Ti_3O_5 crystals up to 3 mm
49	$TiO_{1.67}$	Cl_2 3.3 kPa	1267	1252	10				
47	$TiO_{1.67}$	Cl_2 20 kPa	1267	1252	10				
67, 74	$TiO_{1.75}$	Cl_2 5 kPa	1343	1313	25	0.9	4	5	prisms 3 mm
68, 73	$TiO_{1.80}$	Cl_2 5 kPa	1343	1313	25		5	6	prisms 3 mm
78	$TiO_{1.80}$	Cl_2 5 kPa	1343	1303	22	2.8	5	6	prisms 3 mm
77	$TiO_{1.832}$	Cl_2 5 kPa	1343	1323	22	1.8	6	7	prisms 2 mm
64	$TiO_{1.816}$	Cl_2 5 kPa	1318	1280	24	1.0	6	8	prisms 2 mm
63	$TiO_{1.829}$	Cl_2 5 kPa	1318	1280	24		6	9	prisms 2 mm
61	$TiO_{1.835}$	Cl_2 5 kPa	1289	1233	19	2.0	6 + 8	9	prisms 1 mm

*At T_1: Ti_3O_5 crystals up to 3 mm.

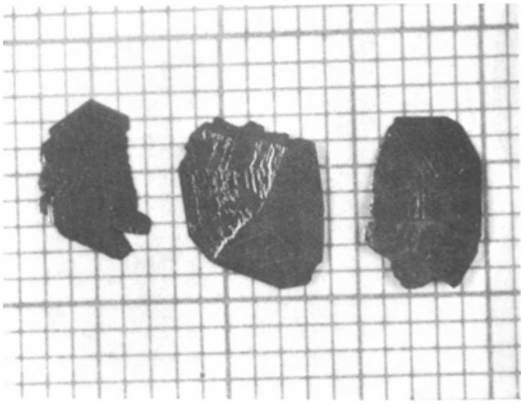

Figure 2 Crystals of Ti_2O_3 from Run 58 (grid in mm).

Ti_4O_7, which seems to be always twinned [19]. Intergrowth of crystals with different values of *n* was observed in one case only, by inspection of the z^* axis. Orientation of a prismatic crystal of Ti_4O_7 in a twin showed that its elongation is parallel to $[45\bar{1}]$. This is consistent with the twin law established by Hodeau *et al.* [19], since $[45\bar{1}]$ is the intersection of the planes $(1\bar{1}\bar{1})$ and (104) which are mirror planes of the pseudo-orthorhombic sublattice governing the twinning. Figs 7 and 8 clearly show the intergrowth of numerous crystallites in Ti_6O_{11} and Ti_9O_{17}. Whereas the large crystals obtained were obviously multiple, we found single crystals of suitable size for X-ray studies [20] for all values of *n* up to 9.

5. Discussion

5.1. Composition shift

We noticed in Run 61 that there was a direct correspondence between the composition shift observed and the equilibrium oxygen vapour pressure, P_O, of the phases obtained at T_1 and T_2 (see Fig. 1). This was then applied to all further runs, aimed at the growth of Ti_5O_9 to Ti_9O_{17}. Theoretical phase shift predictions are shown by horizontal bars in Fig. 1. They are in good agreement with the experimental results given in Table II. This correspondence seems to indicate that thermodynamic equilibrium was reached, and that P_O was constant throughout the tubes in transport Runs 61 to 78.

The oxygen pressure required for these equilibria was $< 10^{-17}$ atm (Fig. 1). The accuracy of the composition shift predictions is therefore somewhat surprising, since the residual pressure in the evacuated transport tubes was about 10^{-8} atm, and since some unreacted TiO_2 (white powder) was found in most runs with $n \geqslant 5$. Our results, however, show that the release of oxygen from other sources in the transport tubes was not significant in our working conditions, which differred from previous works by (a) the use of pure chlorine instead of the moisture-trapping $TeCl_4$ or NH_4Cl, and (b) the synthesis of the starting Ti_nO_{2n-1} phases directly in the transport tubes.

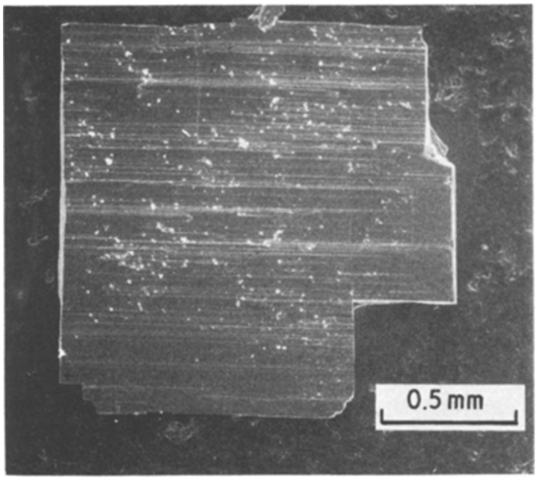

Figure 3 Photomicrograph of a multiple crystal of Ti_3O_5 from the charge zone of Run 49; the striations are parallel to the monoclinic *b*-axis.

Fig. 1 also shows that Ti_2O_3 has a wide range of stability at a given P_O, and hence can be transported without composition shift in temperature gradients of the order of 100 K. The stability range of Ti_3O_5 has a width intermediate between the one of Ti_2O_3 and the much narrower ones of the subsequent phases. Ti_2O_3 and Ti_3O_5, however, require lower equilibrium P_O than the upper

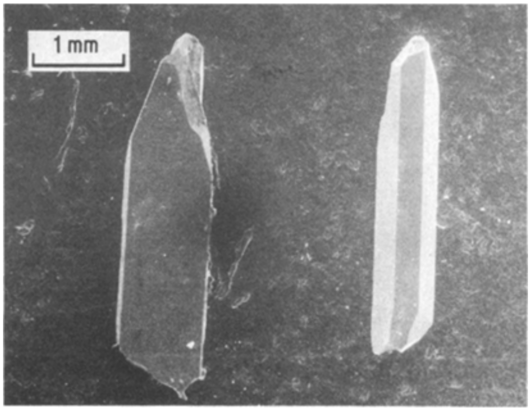

Figure 4 Typical shape of Ti_4O_7 crystals. The elongation is parallel to $[45\bar{1}]$ in one crystallite.

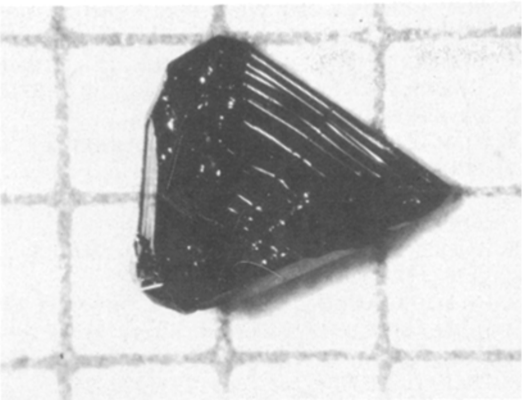

Figure 5 A plate of Ti_4O_7 from Run 47, showing growth step pattern (grid in mm).

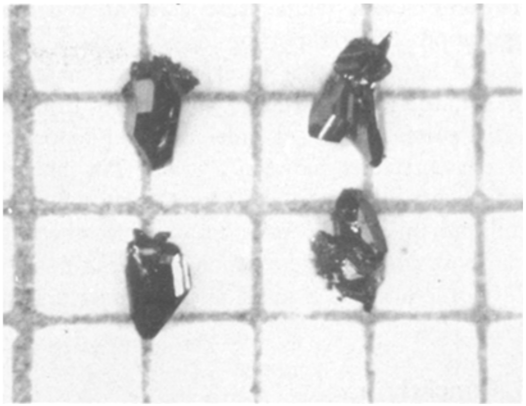

Figure 7 Large multiple crystals of Ti_6O_{11} on the walls of a transport tube (from Run 68).

members of the series at the same temperatures. Consequently, their chemical transport should be more sensitive to residual oxygen or water vapour. Thus in Runs 47, 49 and 53, a starting mixture of composition Ti_3O_5 not only yielded Ti_4O_7 at T_2, but also a mixture of crystals of Ti_3O_5 and Ti_4O_7 at T_1. The theoretical oxygen pressure in these runs (dotted bars on Fig. 1) was of the order of 10^{-22} atm, to be compared to 10^{-17} to 10^{-19} atm for the growth of Ti_nO_{2n-1} with $n \geqslant 5$.

5.2. The transport process

Approximate transport rates (obtained at various temperature gradients) are given in Table II. Both the crystal size and the transport rate tend to decrease as n is increased, in agreement with the thermodynamic data of Table I.

The similarity of the results obtained using chlorine and tellurium tetrachloride is not surprising, since $TeCl_4$ is almost totally dissociated into $TeCl_2 + Cl_2$ at 1300 K [21]. Moreover, tellurium can significantly contaminate titanium oxide crystals during the transport process [11]. Additional problems arise with the use of NH_4Cl, the concentration of which was found to influence directly the oxidation in the hot zone phase [13]. The transport rates obtained with NH_4Cl were comparable to the ones obtained here.

5.3. Crystal growth

The absence of intergrowth of phases with different n values is remarkable. Anderson and Khan [22] reported the existence of an intergrowth structure with $n = 5.5$. The chemical vapour transport of Ti_nO_{2n-1} with $n \geqslant 10$ [13], and of V_9O_{17} in the similar Magneli phase series of vanadium [23] were reported to be beset by intergrowth problems. According to Kuwamoto *et al.* [23], it can be prevented by using very mild conditions for

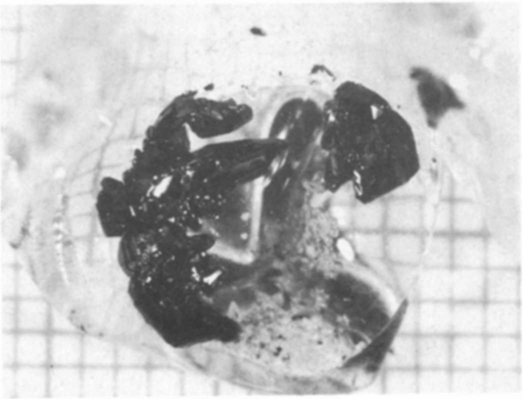

Figure 6 Crystals of Ti_6O_{11} from the charge zone of Run 61 (grid in mm).

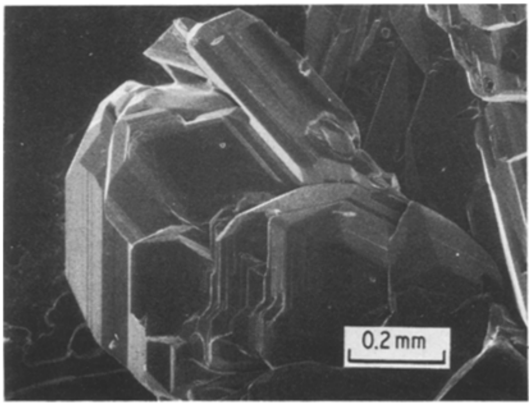

Figure 8 Photomicrograph of intergrown Ti_9O_{17} crystals (from Run 63).

transport (small temperature gradient, low concentration of transporting agent), which were applied here. Another precaution used here was to set the temperature T_2 abruptly from an initial plateau of T_1, in order to avoid deposition of phases stables between T_1 and T_2; this procedure, which favours phase homogeneity but also multiple nucleation, may be valuable when the transport conditions correspond to a composition shift of 2 or more n units, as in Runs 61, 63 and 64.

6. Conclusion

The crystal growth of Ti_nO_{2n-1} oxides is beset by numerous problems, such as their extreme sensitivity to oxygen pressure changes, the low equilibrium constants of their transport reactions, and the possibility of intergrowth. We succeeded here to grow crystals of all members of the series from $n = 2$ to $n = 9$ by chemical vapour transport, taking advantage of the composition shift occurring between different phases maintained at different temperatures in equilibrium with a constant oxygen pressure. Necessary experimental precautions (including the use of chlorine only as a transporting agent) permitted additional oxidation to be minimized and ensured a low transport rate to prevent intergrowth.

Acknowledgement

This paper is published as NRCC contribution No. 20033.

References

1. J. M. HONIG and L. L. VAN ZANDT, *Ann. Rev. Mater. Sci.* 5 (1975) 225.
2. S. ANDERSSON, B. COLLEN, U. KUYLENSTIERNA and A. MAGNELI, *Acta Chem. Scand.* **11** (1957) 1641.
3. L. A. BURSILL and B. G. HYDE, *Prog. Solid State Chem.* 7 (1972) 177.
4. R. F. BARTHOLOMEW and D. R. FRANKL, *Phys. Rev.* 187 (1969) 828.
5. S. LAKKIS, C. SCHLENKER, B. K. CHAKRAVERTY, P. BUDER and M. MAREZIO, *Phys. Rev.* **B14** (1976) 1429.
6. M. MAREZIO, D. TRANQUI, S. LAKKIS and C. SCHLENKER, *ibid.* **B16** (1977) 2811.
7. R. F. BARTHOLOMEW and W. B. WHITE, *J. Crystal Growth* 6 (1970) 249.
8. P. PESHEV and M. IVANOVA, *Phys. Status Solidi* **A28** (1975) K1.
9. G. FOURCAUDOT, J. DUMAS, J. DEVENYI and J. MERCIER, *J. Crystal Growth* **40** (1977) 257.
10. K. NAGASAWA, Y. KATO, Y. BANDO and T. TAKADA, *J. Phys. Soc. Japan* **29** (1970) 241.
11. J. MERCIER and S. LAKKIS, *J. Crystal Growth* **20** (1973) 195.
12. J. J. SINCE, S. AHMED and J. MERCIER, *J. Crystal Growth* **40** (1977) 301.
13. Y. BANDO, S. MURANAKA, Y. SHIMADA, M. KYOTO and T. TAKADA, *ibid.* **53** (1981) 443.
14. I. Z. BABIEVSKAYA, V. A. KRENEV and P. PESHEV, *Mater. Res. Bull.* **14** (1979) 1311.
15. P. STROBEL and Y. LE PAGE, *J. Crystal Growth* **56** (1982) 723.
16. R. M. MERRITT and B. G. HYDE, *Phil Trans. Royal Soc. Lond.* **A274** (1973) 627.
17. D. R. STULL and H. PROPHET (eds.), "JANAF Thermochemical Tables", National Standards Reference Data Series (National Bureau of Standards, Washington DC, 1971) No. 37.
18. Y. LE PAGE and E. J. GABE, *J. Appl. Cryst.* **14** (1981) 117.
19. J. L. HODEAU, M. MAREZIO, C. SCHLENKER, R. BUDER and S. LAKKIS, *ibid.* **9** (1976) 391.
20. Y. LE PAGE and P. STROBEL, *J. Solid State Chem.* **44** (1982).
21. H. OPPERMANN, G. KUNZE and E. WOLF, *Z. Anorg. Allg. Chem.* **434** (1977) 239.
22. J. S. ANDERSON and A. S. KHAN, *J. Less-Common Met.* **22** (1970) 219.
23. H. KUWAMOTO, N. OTSUKA and H. SATO, *J. Solid State Chem.* **36** (1981) 133.

Received 3 December 1981
and accepted 26 January 1982